Optimal Multiple-Impulse Direct Ascent Fixed-Time Rendezvous

LARRY R. GROSS*
Air Force Aero Propulsion Laboratory, Wright-Patterson Air Force Base, Ohio
AND
JOHN E. PRUSSING†
University of Illinois, Urbana, Ill.

Minimum-fuel, impulsive, direct ascent rendezvous trajectories are obtained for the fixed transfer time case. The terminal orbit is circular about a spherical nonrotating planet. The inclination and radius of the terminal orbit, the target position at launch, and the transfer time are independent parameters in the problem. Two- and three-impulse optimal solutions are obtained. The primer vector evaluated along a nonoptimal trajectory provides a gradient of the cost with respect to impulse times and locations. The Davidon-Fletcher-Powell algorithm is used to perform the minimization. For certain rendezvous geometries and transfer times the optimal three-impulse time-fixed fuel cost is lower than the optimal two-impulse time-open cost.

I. Introduction

THE problem of minimum-fuel impulsive trajectories in an inverse square gravitational field has a well-developed theory stemming from Lawden's initial work.[1] This study is a particular case of Lawden's Problem, involving minimum-fuel, multiple-impulse, direct ascent trajectories for which the transfer time is fixed.

In a survey article by Gobetz and Doll[2] the known results (1969) are cited for Lawden's Problem, including direct ascent rendezvous. A recommendation of the survey is that further research in fixed-time optimal multiple-impulse rendezvous be done. It is in the spirit of that recommendation that this study was undertaken. The present article summarizes the results of Ref. 3.

For the time-free case, Carstens and Edelbaum[4] and Haviland and House[5] have found the fuel-optimal two-impulse elliptical transfer for a direct ascent from an arbitrary launch point on a spherical nonrotating planet or moon to an equatorial circular orbit. Carstens and Edelbaum compared this two-impulse result to a nonoptimal three-impulse trajectory consisting of a circular parking orbit at the planet surface, followed by an inclined Hohmann transfer to the final orbit. For some rendezvous geometries this nonoptimal three-impulse transfer requires less fuel than the optimum two-impulse transfer.

Results for optimal fixed-time direct ascent trajectories are very limited; however, a theoretical study of the optimal fixed-time impulsive problem by Lion and Handelsman[6] and an application of their results to orbital rendezvous by Jezewski and Rosendaal[7] provide a basis for this investigation.

The objectives of this paper are twofold. First, to present a brief description of a method for obtaining fixed-time, minimum-fuel, multiple-impulse trajectories based on Ref. 6. Second, to present results for the particular problem of optimal fixed-time direct ascent two- and three-impulse rendezvous with a target vehicle in an arbitrary circular orbit. The assumptions made are that the planet or moon is spherical and nonrotating, and that atmospheric forces are negligible. The interceptor spacecraft velocity relative to the planet is considered to be zero before first impulse.

Received July 30, 1973; revision received January 22, 1974. This paper was also presented at the AAS/AIAA Astrodynamics Conference, Vail, Colo., July 16–18, 1973.

Index category: Spacecraft Navigation, Guidance, and Flight-Path Control Systems.

* Chief of Propulsion Branch.

† Associate Professor, Aeronautical and Astronautical Engineering Department. Member AIAA.

II. Description of the Method

The necessary conditions for an optimal impulsive transfer in terms of the primer vector, **p**, the vector of adjoint variables associated with the velocity vector, are well documented.[1,6] The primer vector satisfies the linear differential equation

$$\ddot{\mathbf{p}} = G(\mathbf{r})\mathbf{p} \tag{1}$$

where G is the gravity gradient matrix evaluated along the orbit $\mathbf{r}(t)$ being tested for optimality. The basic conditions for an optimal impulsive transfer are that the primer vector magnitude, p, never exceed unity and that the impulses be applied in the direction of the vector **p** at those times for which $p = 1$.

Lion and Handelsman[6] have demonstrated that the primer along a nonoptimal trajectory provides information indicating how that trajectory can be improved. For an n-impulse trajectory, cost is incurred only at each impulse point, and the cost functional can be expressed in terms of the discontinuously altered velocities at each impulse time, t_k:

$$J = \sum_{k=1}^{n} |\Delta\mathbf{V}(t_k)|; \qquad k = 1, 2, \ldots, n \tag{2}$$

At each impulse along an optimal trajectory, the primer is a unit vector aligned with the velocity change

$$\mathbf{p}(t_k) = \Delta\mathbf{V}(t_k)/\Delta V(t_k) \tag{3}$$

If the velocity changes on any two-impulse segment of a multiple-impulse trajectory are known, then the primer values at the ends of that segment are known. Using the transition matrix for the solution to Eq. (1), the primer rate can be determined for either end point of the segment by[6]

$$\dot{\mathbf{p}}(t_k) = N^{-1}(t_{k+1}, t_k)\,[\mathbf{p}(t_{k+1}) - M(t_{k+1}, t_k)\mathbf{p}(t_k)] \tag{4}$$

where the transition matrix has been partitioned into

$$\Phi(t_{k+1}, t_k) = \begin{bmatrix} M(t_{k+1}, t_k) & N(t_{k+1}, t_k) \\ S(t_{k+1}, t_k) & T(t_{k+1}, t_k) \end{bmatrix} \tag{5}$$

The primer and its rate at a particular time, say t_k, provide the necessary boundary conditions to determine the complete primer solution over the entire segment. The transition matrix [Eq. (5)] for the primer vector is identical to that for the two-body variational equations; the form developed by Stern[8] is used in this study.

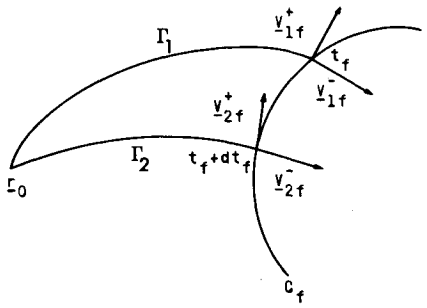

Fig. 1 Schematic for comparing two-impulse and two-impulse with final coast trajectories.

Primer Vector on Nonoptimal Trajectories

Lion and Handelsman[6] extended the definition of the primer vector to a nonoptimal two-impulse segment of a trajectory by defining it to be the solution of Eq (1) with boundary conditions

$$\mathbf{p}(t_k) = \Delta\mathbf{V}(t_k)/\Delta V(t_k) \tag{6}$$

$$\mathbf{p}(t_{k+1}) = \Delta\mathbf{V}(t_{k+1})/\Delta V(t_{k+1}) \tag{7}$$

By examining the primer solution along a nonoptimal trajectory the conditions can be found for which a final coast or the addition of a midcourse impulse would yield a first-order decrease in the cost. A schematic of comparison trajectories is given in Figs. 1 and 2, where C_f is the final (target) orbit. The equation equation for the first-order change in cost due to a final coast (trajectory Γ_2 of Fig. 1) is given by

$$dJ = \dot{\mathbf{p}}_f^T(-d\mathbf{r}_f + \mathbf{V}_{1f}^- dt_f); \qquad dt_f < 0 \tag{8}$$

The subscript f denotes conditions at the final time.

The first-order change in cost in those cases in which the addition of an impulse will lower the cost (Fig. 2) is given by

$$dJ = (\dot{\mathbf{p}}_m^+ - \dot{\mathbf{p}}_m^-)^T d\mathbf{r}_m - (\dot{\mathbf{p}}_m^{+T}\mathbf{V}_{1m}^+ - \dot{\mathbf{p}}_m^{-T}\mathbf{V}_{1m}^-)dt_m \tag{9}$$

The subscript m denotes conditions at the midcourse impulse time.

The coefficients of $\mathbf{dr}$ and dt in the two preceding equations are components of the gradient of the cost with respect to the position, $\mathbf{r}$, and time t of an impulse. Both equations are of the form

$$dJ = \mathbf{g}^T\mathbf{dy}; \qquad \mathbf{dy}^T \triangleq [d\mathbf{r}^T\, dt] \tag{10}$$

Thus, once the primer rates are computed the gradient vector $\mathbf{g}$ is available for use in a first-order numerical minimization scheme to minimize the cost J. The scheme used in this study was Davidon-Fletcher-Powell. The algorithm iterates on the four parameters (three components of $\mathbf{r}$ and the variable t at either the midcourse time or the final time) until the cost J is minimized ($\mathbf{g} \cong \mathbf{0}$).

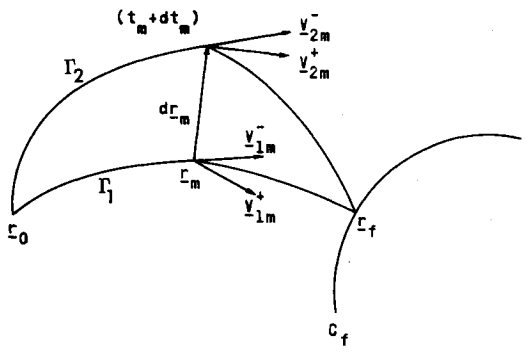

Fig. 2 Schematic for comparing three-impulse trajectories.

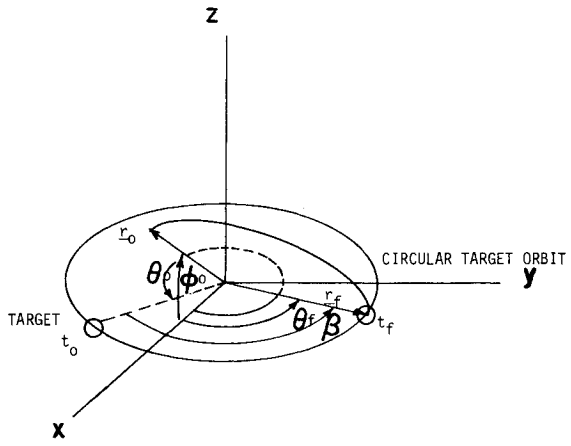

Fig. 3 Rendezvous geometry.

The procedure for obtaining optimal trajectories is the following: for each final orbit and launch point, generate candidate two-impulse primer solutions by incrementing the rendezvous point in the final orbit. From the primer solutions identify those trajectories which yield optimal two-impulse solutions and those which indicate that the trajectory can be improved by a final coast or an additional impulse. In the latter cases add the required coast or impulse and use the improved trajectory as a starting condition in the numerical minimization scheme.

On each two-impulse segment Lambert's problem is solved for the elliptic arc connecting the given end points in the specified time interval. The required ΔV's are obtained by subtracting velocities on each side of the impulse points. The primer vector and its rate are determined by using the transition matrix Eq. (5) with boundary conditions given in Eqs. (3) and (4).

III. Rendezvous Geometry and Units

The previously described procedure can be applied to the specific problem of determining the two- and three-impulse rendezvous trajectories that connect an initial point at the planet's surface to a target in a circular orbit. The fixed transfer time for the rendezvous trajectory is then defined by the target's travel time from its position at the initial time to a specific rendezvous position.

The rendezvous geometry is shown in Fig. 3. The launch point lies in the xz plane while the target orbit lies in the xy plane. This choice of coordinate frame orientation is merely a convenient one, it does not affect the generality of the results. From the given geometry, individual optimal trajectories can be categorized according to the radius of the final orbit r_f, the latitude of the launch point, ϕ_o, the target's initial longitude, θ_o, and the angular distance traveled by the target to complete rendezvous, β. For simplicity, the angle β which is defined by the target's initial and rendezvous position vectors is called the travel angle. The travel angle is a normalized measure of the transfer time.

The units for position, velocity and time used in this analysis are chosen so that the gravitational constant, μ, has unit magnitude. r_f is in units of the planet radius and velocity is in units of circular speed at the planet surface.

IV. Results

The relative usefulness of an optimal fixed-time impulsive rendezvous trajectory can be evaluated by comparing its ΔV cost to that of the corresponding time-free, optimal two-impulse trajectory, since this is the best possible two-impulse trajectory if transfer time and rendezvous position are not specified. Using the time-free transfer requires that the spacecraft waits at the launch point until the target reaches exactly the proper initial position which will allow rendezvous at the optimal final position in the specified transfer time.

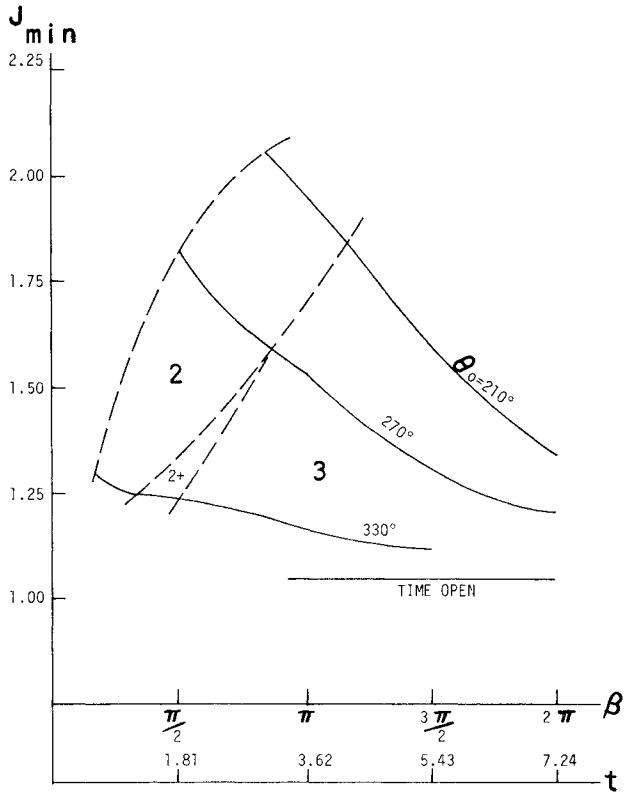

Fig. 4 Optimal cost vs target travel angle, $r_f = 1.1$, $\phi_o = 0$.

In addition to the time-free, two-impulse trajectory, a non-optimal three-impulse trajectory is used for comparison in this analysis. The comparison three-impulse trajectory consists of a circular trajectory along the planet surface starting at the launch point and ending at the positive y axis followed by an inclined Hohmann ellipse that meets the final orbit at the negative y axis. The inclination angle of the Hohmann ellipse plane with respect to the final orbit (xy) plane is equal to the latitude of the launch point. This particular three-impulse trajectory is used for comparison because Carstens and Edelbaum[4] demonstrated that it has lower cost than the time-free, two-impulse optimal trajectory if the radius of the final circular orbit is large and if the latitude of the launch point is small.

The ΔV cost of the optimal two and three impulse rendezvous trajectories as a function of target travel angle is shown in Figs. 4–9. Each figure presents the minimum cost for a particular final orbit radius and launch point latitude as a function of the fixed transfer time (the target travel angle, β), with target initial longitude as a parameter. The dashed lines are the boundaries separating the optimal two-impulse trajectories (2), optimal two-impulse trajectories with final coast (2^+), and optimal three-impulse trajectories (3). The circle-to-Hohmann cost is not shown on the figures with ϕ_o equal to zero because it is disproportionately higher than the two-impulse, time-free cost. The two-impulse trajectories are bounded on the left to exclude those trajectories with insufficient transfer time to allow the radial position to be greater than the planet radius at all points.

The optimal three-impulse rendezvous trajectories provide lower cost than the corresponding optimal two-impulse, time-free trajectories typically for large launch point latitude (60°). The three-impulse trajectories present a maximum cost advantage of approximately 4% for a final orbit radius 1.1 and 2% for a final orbit radius of 2.0 for the range of transfer times investigated. As expected, the ΔV cost of both the two- and three-impulse optimal rendezvous trajectories decreases as the transfer time increases; the two-impulse rendezvous trajectories never have a lower cost than the corresponding two-impulse, time-free trajectory. One interesting trend is that a two-impulse trajectory followed by a final coast is never an optimal solution if the target initial longitude is 210° or 270°.

A two-impulse with final coast solution is optimal for a range of transfer times for an initial target longitude of 330°. The two-impulse with final coast solutions use the transfer corresponding to the preceding optimal two-impulse trajectory, followed by a coast in the final orbit for the remaining transfer time. The final coast does not change the ΔV cost because the rendezvous is

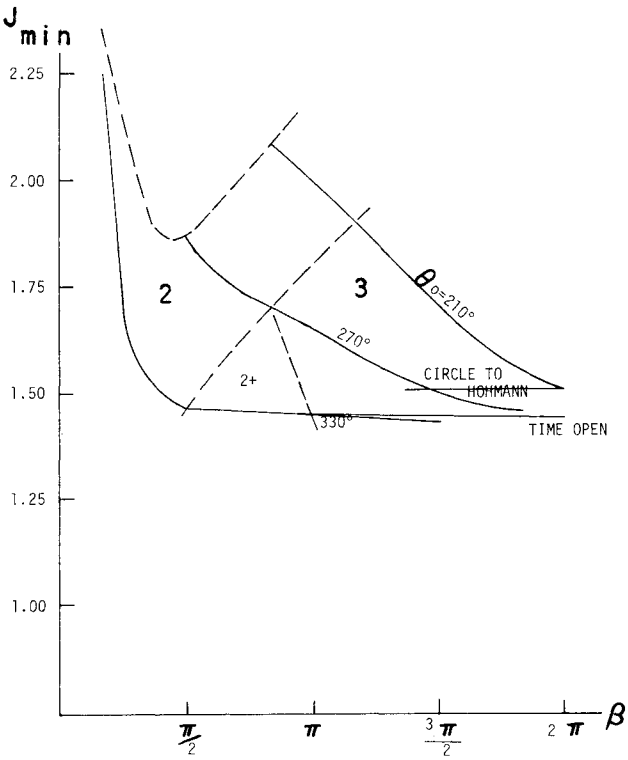

Fig. 5 Optimal cost vs target travel angle, $r_f = 1.1$, $\phi_o = 30$.

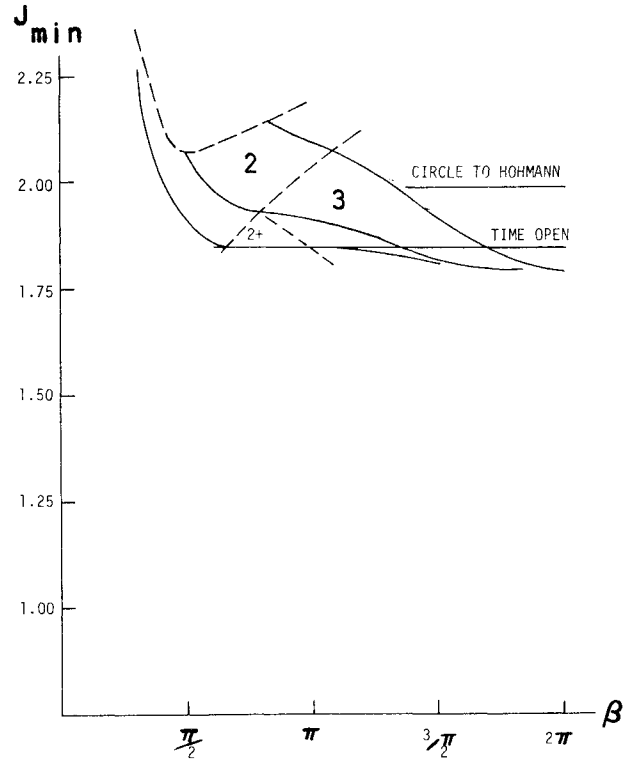

Fig. 6 Optimal cost vs target travel angle, $r_f = 1.1$, $\phi_o = 60$.

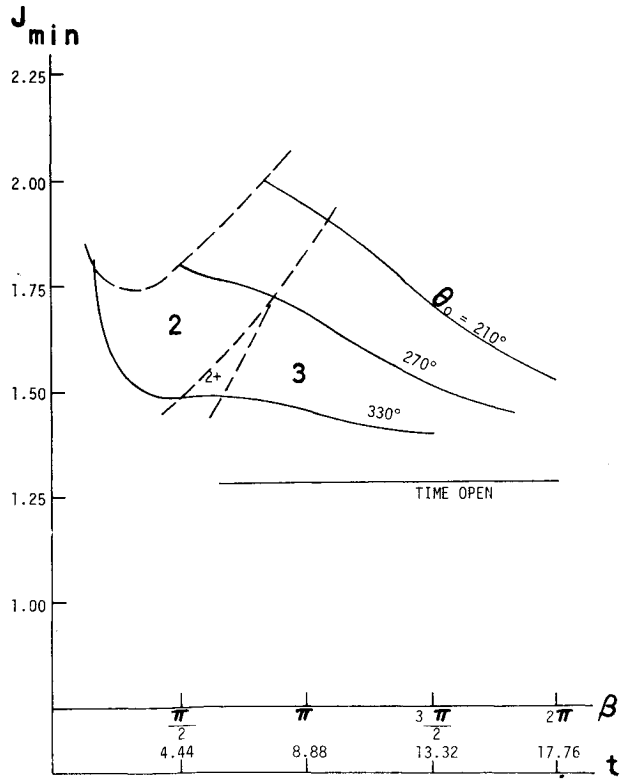

Fig. 7 Optimal cost vs target travel angle, $r_f = 2.0$, $\phi_o = 0$.

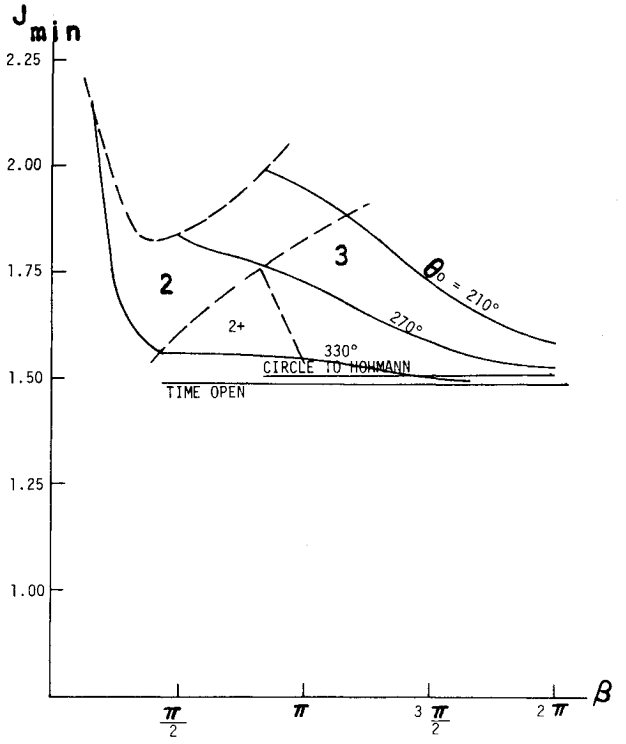

Fig. 8 Optimal cost vs target travel angle, $r_f = 2.0$, $\phi_o = 30$.

complete. The two-impulse with final coast solutions either equal or exceed the cost of the time-free, two-impulse optimal solutions depending on whether the initial geometry and transfer time permit rendezvous at the optimal final position in the optimal transfer time.

V. Example Three Impulse Trajectory

Figure 10 shows the optimal three-impulse trajectory obtained for a launch point latitude of 60° and a final orbit radius of 1.1 when the target travels one full revolution. The pertinent orbital parameters are listed in the figure.

At the time of the initial impulse, the target is at a 210° longitude. The initial impulse establishes an elliptical trajectory of moderate eccentricity that is inclined 62.6° with respect to the xy plane. At the midcourse impulse time, the target has traveled 194.8° along its circular orbit, while the rendezvous vehicle has traveled 13.4° past apoapse and has intersected the xy plane. The midcourse impulse magnitude and direction is applied to cancel the z component of velocity and adjust the x and y components to correspond to the initial velocity required on the second elliptical trajectory, Γ_2. Γ_2 is less eccentric and slightly larger than Γ_1. The rendezvous vehicle arrives nearly tangentially at the circular target orbit. Since the rendezvous vehicle's position on Γ_2 is very close to periapse, its velocity is larger than the corresponding circular velocity of the target. The final impulse adjusts the vehicle's velocity by canceling its radial component of velocity and reducing its tangential component of velocity.

VI. Summary

This study demonstrates the use of the primer vector to provide gradient information for use in a first-order numerical minimization scheme for minimum-fuel impulsive trajectories.

The results indicate that the optimal two-impulse, time-free trajectory has a lower ΔV cost than optimal three-impulse rendezvous trajectories over a wide range of transfer times and target initial longitudes for low launch point latitudes (0° and 30°). An exception occurs for $R_f = 1.1$, $\theta_o = 330°$, and $\beta \geqq 180°$, in which the three-impulse rendezvous provides a smaller cost.

However, for larger launch point latitudes (60°) the optimal three-impulse rendezvous trajectories provide a cost reduction relative to the optimal two-impulse time-free trajectory over a wide range of transfer times and target initial longitudes.

A two-impulse trajectory followed by a final coast is typically the optimal trajectory for an intermediate range of transfer times and a large enough target initial longitude (see the 330° case).

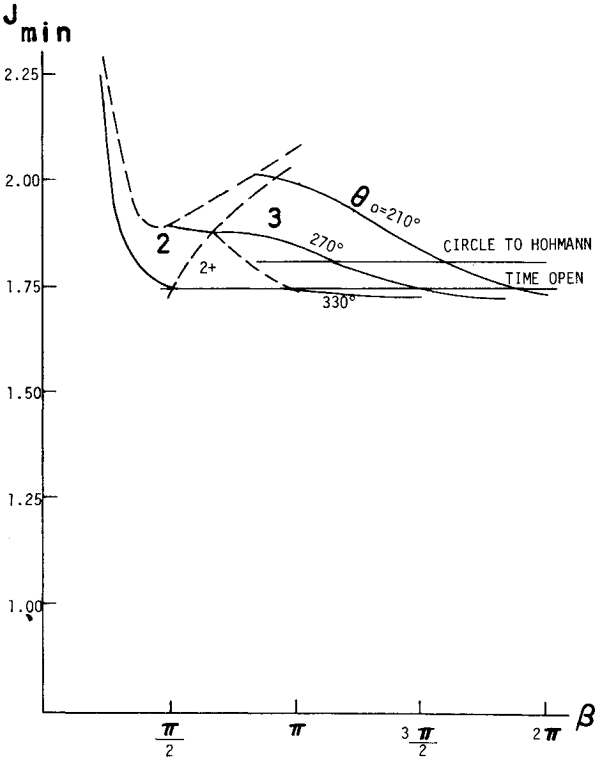

Fig. 9 Optimal cost vs target travel angle, $r_f = 2.0$, $\phi_o = 60$.

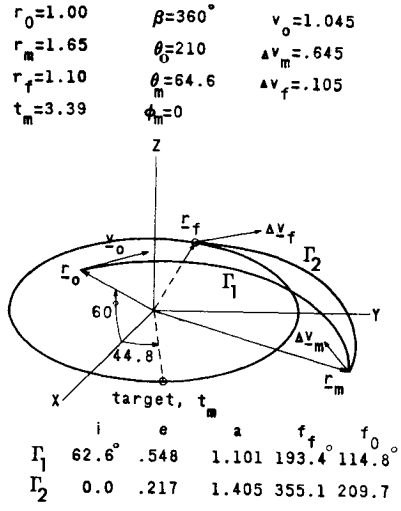

Fig. 10 Example three-impulse rendezvous trajectory.

The position vector of the midcourse impulse for the optimal three-impulse trajectory typically has a magnitude larger than the target radius and a longitude larger than the target longitude at the midcourse time. The latitude of the midcourse impulse position is generally a small angle which tends to zero as the transfer time and final longitude increase. The interceptor vehicle is then typically positioned above and in front of the target at the optimal midcourse impulse.

References

[1] Lawden, D. F., *Optimal Trajectories for Space Navigation*, Butterworths, London, 1963.

[2] Gobetz, F. W. and Doll, J. R., "A Survey of Impulsive Trajectories," *AIAA Journal*, Vol. 7, No. 5, May 1969, pp. 801–834.

[3] Gross, L. R., "Optimal Multiple-Impulse Direct Ascent Rendezvous," Ph.D. thesis, 1972, Univ. of Illinois, Urbana-Champaign, Ill.

[4] Carstens, J. P. and Edelbaum, T. N., "Optimum Maneuvers for Launching Satellites into Circular Orbits of Arbitrary Radius and Inclination," *ARS Journal*, Vol. 31, No. 7, July 1961, pp. 943–949.

[5] Haviland, R. P. and House, C. M., "Nonequatorial Launching to Equatorial Orbits and General Nonplanar Launching," *AIAA Journal*, Vol. 1, No. 6, June 1963, pp. 1336–1342; also "Addendum," *AIAA Journal*, Vol. 1, No. 9, Sept. 1963, p. 2197.

[6] Lion, P. M. and Handelsman, M., "Primer Vector on Fixed-Time Impulsive Trajectories," *AIAA Journal*, Vol. 6, No. 1, Jan. 1968, pp. 127–132.

[7] Jezewski, D. J. and Rozendaal, H. L., "An Efficient Method for Calculating Optimal Free-Space N-Impulse Trajectories," *AIAA Journal*, Vol. 6, No. 11, Nov. 1968, pp. 2160–2165.

[8] Stern, R. G., "Interplanetary Midcourse Guidance Analysis," MIT Sc.D. thesis, 1963, Dept. of Aeronautics and Astronautics, MIT, Cambridge, Mass.

JULY 1974 AIAA JOURNAL VOL. 12, NO. 7

Liapunov Stability Analysis of Hybrid Dynamical Systems in the Neighborhood of Nontrivial Equilibrium

LEONARD MEIROVITCH*
Virginia Polytechnic Institute and State University, Blacksburg, Va.

This paper is concerned with the stability of a hybrid dynamical system in the neighborhood of a nontrivial equilibrium, where the system consists of one rigid part and n elastic members. The body moves in a central-force field with its mass center describing a circular orbit. The nontrivial equilibrium is defined by steady rotation of the system at an angular velocity equal to the orbital velocity, with the elastic members being in deformed state. A Liapunov stability analysis is performed by assuming small perturbations about the nontrivial equilibrium, where the latter is generally defined by nonlinear differential equations. The theory is applied to a gravity-gradient stabilized satellite with flexible appendages.

Introduction

WITH the advent of large orbiting spacecraft, the flexibility effect has become increasingly significant, as it can alter appreciably the stability characteristics of the system. This is particularly true of hybrid dynamical systems with extremely flexible elastic members, where a hybrid system is defined as one described by both ordinary and partial differential equations.

The stability of hybrid dynamical systems has received considerable attention in the last few years.[1–5] In all these works the equilibrium configuration was the trivial one, namely, that in which the elastic members are in undeformed state. The assumption of trivial equilibrium is reasonable if the elastic members are aligned with the body principal axes when in undeformed state. However, if the elastic members are not aligned with the body principal axes, then the equilibrium configuration need no longer be trivial.[6] Reference 6 is concerned with the shape of the flexible members in the equilibrium configuration. The solution of the nonlinear differential equations of Ref. 6 was obtained by means of an analog computer. The equilibrium alone is investigated more extensively in two reports (Refs. 7 and 8), with the results obtained by means of a digital computer program being presented in Ref. 8.

Presented at the AAS/AIAA Astrodynamics Conference, Vail, Colo., July 16–18, 1973; received July 27, 1973; revision received January 17, 1974. This investigation was supported by the NASA Research Grant NGR 47-004-098 sponsored by the Stabilization and Control Branch, Goddard Space Flight Center. The author has benefited appreciably from discussions with J. V. Fedor of NASA Goddard Space Flight Center. The numerical results have been obtained by means of a computer solution written by J.-N. Juang, a graduate student in the Department of Engineering Science and Mechanics, Virginia Polytechnic Institute and State University.

Index categories: Spacecraft Attitude Dynamics and Control; Structural Dynamic Analysis.

* Professor, Department of Engineering Sciences and Mechanics. Associate Fellow AIAA.